Theoretical study on the relationship between the position of the substituent and the ESIPT fluorescence characteristic of HPIP*

Xin Zhang(张馨), Jian-Hui Han(韩建慧), You Li(李尤), Chao-Fan Sun(孙朝范),
Xing Su(苏醒), Ying Shi(石英)†, and Hang Yin(尹航)‡

Institute of Atomic and Molecular Physics, Jinlin University, Changchun 130012, China

The influences of the substituent base position on the excited state intramolecular proton transfer fluorescence properties were explored in 2-(2′-hydroxyphenyl)imidazo[1,2-*a*]-pyridine (HPIP) and HPIP's derivatives (5′Br-HPIP and 6′Br-HPIP). And the density functional theory (DFT) and time-dependent DFT (TD-DFT) methods were used to calculate the molecule structures. The calculated results showed that the influence of 5′Br-HPIP on the fluorescence intensity is stronger than that of 6′Br-HPIP. The fluorescence emission peak of 5′Br-HPIP occurred a blue shift compared with HPIP, and 6′Br-HPIP exhibited an opposite red shift. The change of the fluorescence emission peak was attributed to the decrease of the energy gap from 6′Br-HPIP to 5′Br-HPIP. Our work on the substituent position influence could be helpful to design and develop new materials.

1. Introduction

Fluorescent organic materials have been attracting considerable interest in various application fields because their benefit properties, such as sensibility,[1–5] good specificity,[6,7] wide range of linear analysis, and easy to handle.[8–11] A huge number of organic molecules exhibit excited state intramolecular proton transfer (ESIPT) properties. ESIPT is a light induced ultrafast phenomenon that the proton transfers from the donor to acceptor portion upon optical excitation.[12–20] A large Stoke shift can be observed in the ESIPT process.[21] Through special photo-excitation, the molecule with ESIPT characteristics usually shows a dual fluorescence phenomenon.[21,22] The fluorescence peak generated before the proton transfer is called normal fluorescence, and that derived after the proton transfer is named ESIPT fluorescence.[23] The characteristics of ESIPT fluorescence are closely related to the molecule structure.[24–27] Most organic molecules all show effective ESIPT fluorescence and have a high quantum field in fluid solvent.[28] Moreover, with the progress of experiment, the method of changing the ESIPT characteristic by modifying the structure of the original molecule has also been applied in many fields in recent years.[29,30] Besides, many researches proved that both intermolecular and intramolecular interactions could influence the ESIPT process.[31,32] The enhancement of the hydrogen bond strength will promote the intramolecular ESIPT process. Upon the photo-induce process, the electron densities of the proton donor group and acceptor group will reduce and increase, re-

spectively. Therefore the transfer process will be facilitated in the S_1 state.[33–36]

Recently, an organic luminescent material, the 2-(2′-hydroxyphenyl)imidazo[1,2-*a*]-pyridine (HPIP) has been attracting considerable attraction. As a representative member of pyridyls family, HPIP is well known for its special fluorescence property. Unlike many organic molecules, HPIP usually shows weak fluorescence in solvent. In Yasuhiro *et al.*'s study, they summarized that the conical intersection (CI) led to the weak quantum yield of fluorescence in solution.[37] In Swatain *et al*.'s study, they synthesized various HPIP derivatives (HPIPs), compared the effects of 5′-substituded HPIPs and 6′-substituded HPIPs on the molecule properties, and found that different substitution position influenced the ESIPT fluorescence emission peak's red or blue shift.[38] However, the relationship between the position of the substitution group and the fluorescence intensity is still unclear.

In the present work, we investigate the HPIP, 5′Br-HPIP, and 6′Br-HPIP molecules theoretically aiming at exploring the ESIPT process, the property of intramolecular hydrogen bonds, and the dynamic behaviors of the three compounds. Hereinto, the structures of the three molecules in S_0 state and S_1 state are optimized by the density functional theory (DFT) method and the time-dependent DFT (TDDFT) method, respectively. The primary hydrogen bond lengths of the three compounds are calculated. In addition, the infrared (IR) vibrational spectra in ground-state and excited-state, absorption and emission spectra of the three molecules are studied. Moreover, the reduced density gradient (RDG) function, frontier molecu-

†Corresponding author. E-mail: shi_ying@jlu.edu.cn
‡Corresponding author. E-mail: yinhang@jlu.edu.cn

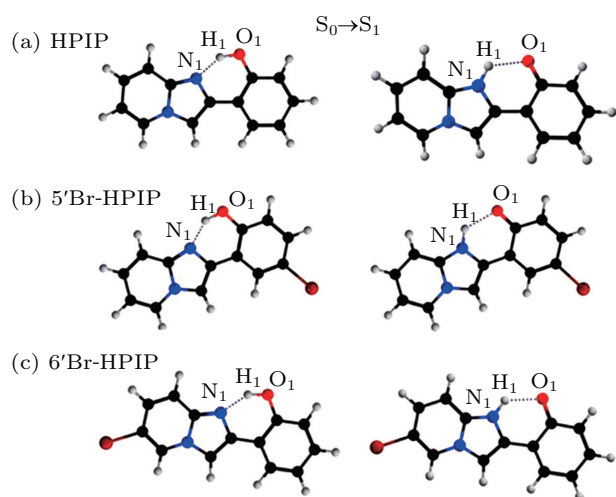lar orbitals analysis (FMOs), and potential energy curve (PEC) of the three molecules are also investigated.

2. Method

In this work, the related calculations were completed on the Gaussian 09 program suit.[39] For making the theoretical value consistent with the experimental one, we used different functions (B3LYP, M062X, Cam-B3LYP, and PBE0) to calculate the ground-stated property of the compounds. The geometrical framework of the compound was optimized by the DFT method in ground-state and the TDDFT method in excited-state, respectively.[40–42] The tetrahydrofuran (THF) solvent with integral equation formalism variant of polarizable continuum model (IEFPCM) was used in theoretical arithmetic. The calculation of the non-covalent interactions by RDG function was executed using the Multiwfn program.[43] Chemcraft software was exploited to visualize the RDG in a real place.[44]

3. Results and discussion

3.1. Optimized geometric structure

To analyzed the intramolecular hydrogen bond interaction of the three molecules, we optimized structures of HPIP, 5′Br-HPIP, and 6′Br-HPIP by B3LYP/6-31G(d) in ground-state and excited-state. The energy of S_1 state was the lowest of all excited states, the structure of S_1 state was the most stable structure in all excited-state structures. So we optimized the structure at S_1 state of the three molecules. And the structures of three molecules are displayed in Fig. 1.

Fig. 1. Optimized structures of (a) HPIP, (b) 5′Br-HPIP and, (c) 6′Br-HPIP in S_0 state and S_1 state, with C atoms (black), H atoms (gray), O atoms (red), N atoms (blue), and Br atoms (crimson).

The bond lengths of HPIP, 5′Br-HPIP, and 6′Br-HPIP in ground-state and excited-state are shown in Table 1. The bond length of O_1–$H_1 \cdots N_1$ in HPIP changed from 1.01 Å in the S_0 state to 1.99 Å in the S_1 state, and the bond length of N_1–$H_1 \cdots O_1$ decreased from 1.64 Å in the S_0 state to 1.01 Å in

the S_1 state. Moreover for 5′Br-HPIP, the bond lengths of O_1–$H_1 \cdots N_1$ and N_1–$H_1 \cdots O_1$ changed from 1.02 Å, 1.63 Å in ground-state to 1.93 Å, 1.01 Å in excited-state, respectively. For 6′Br-HPIP, the bond lengths of O_1–$H_1 \cdots N_1$ and N_1–$H_1 \cdots O_1$ transformed from 1.02 Å, 1.90 Å in S_0 state to 1.65 Å, 1.02 Å in S_1 state, respectively. From the results, the intramolecular hydrogen bond interaction between N_1 and H_1 was enhanced in S_1 state for the three molecules. The phenomenon indicated the occurrence of ESIPT process.

Table 1. Calculated important bond lengths (Å) for the optimized structure of HPIP, 5′Br-HPIP, and 6′Br-HPIP in ground-state (S_0) and excited-state (S_1).

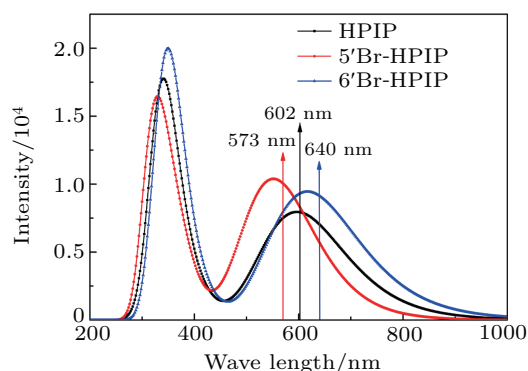|		O_1–$H_1 \cdots N_1$	N_1–$H_1 \cdots O_1$
HPIP	S_0	1.01	1.64
	S_1	1.99	1.01
5′Br-HPIP	S_0	1.02	1.63
	S_1	1.93	1.01
6′Br-HPIP	S_0	1.02	1.65
	S_1	1.90	1.02

3.2. Absorption and emission spectra

Table 2 shows the experimental[38] and theoretical absorption peaks of HPIP, 5′Br-HPIP, and 6′Br-HPIP. The theoretical values were calculated by different functions (M062X, B3LYP, CAM-B3LYP, and PBE0) with 6-31G(d) basis set. From the results, the values of B3LYP were in good agreement with the experimental ones,[38] and affirmed the dependability of our computational method. In addition, the corresponding oscillator strengths of two excited-states for the three molecules were also calculated. The oscillator strength in S_1 state was 0.35, 0.36, and 0.34 for HPIP, 5′Br-HPIP, and 6′Br-HPIP, respectively. And the oscillator strength in S_2 state was 0.004, 0.003, and 0.020 for HPIP, 5′Br-HPIP, and 6′Br-HPIP, respectively. The results displayed that the S_1 state oscillator strength was stronger than the S_2 state oscillator strength. The transition $S_0 \rightarrow S_1$ of the three molecules was considered in the present system.

Table 2. Experimental and theoretical arithmetic absorption peaks (nm) of HPIP, 5′Br-HPIP, and 6′Br-HPIP by different functional methods.

	HPIP	5′Br-HPIP	6′Br-HPIP
B3LYP	327.63	326.91	340.79
Exp.[38]	341	333.5	341
M062X	283.35	285.60	285.79
CAM-B3LYP	286.70	288.10	288.06
PBE0	395.47	399.91	558.82

The calculated emission spectra of the three molecules are shown in Fig. 2. The calculated value was in accordance with the experimental one.[38] In addition, HPIP, 5′Br-HPIP, and 6′Br-HPIP showed dual fluorescence emission. The near-UV emission belonged to normal fluorescence, and the other one was assigned to ESIPT fluorescence.[38] The normal fluorescence emission regions of the three molecules were similar.[38] And for the ESIPT fluorescence emission peak,

5′Br-HPIP showed a blue shift compared with HPIP, and 6′Br-HPIP occurred an opposite red shift. Moreover, different substituent position could influence the ESIPT fluorescence intensity. The fluorescence intensity of 5′Br-HPIP was 11.84% higher than HPIP's fluorescence intensity, and 6′Br-HPIP was 3.02% higher than HPIP in fluorescence intensity. The results indicated that different substituent position could influence the ESIPT fluorescence properties.
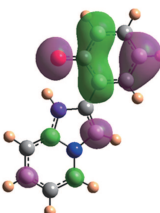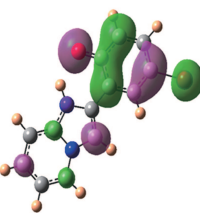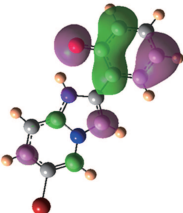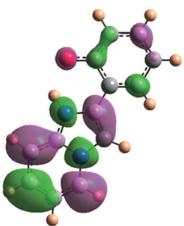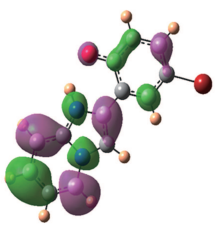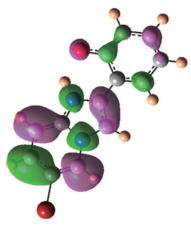

Fig. 2. Theoretical fluorescence emission spectra of HPIP (black line), 5′Br-HPIP (red line), and 6′Br-HPIP (blue line). The arrowheads represent the experimental value of the emission peak of HPIP (black), 5′Br-HPIP (red), and 6′Br-HPIP (blue), respectively.[38]

3.3. Frontier molecular orbitals analysis

As we know, FMO analysis is an significant way to gain the charge distribution changes in molecule at the excited transition.[45] Table 3 shows the highest occupied molecular orbital (HOMO) and the lowest unoccupied molecular orbital (LUMO) of the three molecules in S_1 state. The π character of HOMO and π^* character of LUMO appeared in the three molecules. This result presented the $\pi\pi^*$-type feature of the transition from S_0 to S_1 state. The charge transfer from HOMO to LUMO of the three molecules was analogous. From HOMO to LUMO, the density distribution of O_1 atoms decreased and the density distribution of N_1 atoms increased in the three molecular structures. The results indicated that the electronegativity of N_1 atoms was stronger than that of O_1 atoms. The interaction between N_1 and H_1 was strengthened which caused the occurrence of ESIPT process. The calculated results showed that the energy level of HOMO was -1.96 eV (HPIP), -2.04 eV (5′Br-HPIP), and -2.22 eV (6′Br-HPIP). Moreover, the LUMO energy level was -4.56 eV (HPIP), -4.72 eV (5′Br-HPIP), and -4.65 eV (6′Br-HPIP), respectively. Furthermore, the energy gaps of the three molecules followed the order 5′Br-HPIP (2.68 eV)> HPIP (2.60 eV)> 6′Br-HPIP (2.43 eV), which corresponded to the change of ESIPT fluorescence emission peak in Fig. 2. Moreover, the energy gap of 5′Br-HPIP was larger than that of 6′Br-HPIP, indicating that 5′substituent position showed a stronger influence on the ESIPT fluorescence property than 6′substituent position.

Table 3. Frontier molecular orbitals (HOMO and LUMO) of HPIP, 5′Br-HPIP, and 6′Br-HPIP structures.

	HPIP	5′Br-HPIP	6′Br-HPIP
HOMO			
LUMO			

3.4. Non-covalent interactions analysis

Yang *et al.* advanced a way to imagine non-covalent interactions in real space, which could explore hydrogen bond characteristics.[46,47] The analysis of electron density ($\rho(r)$) and the reduced density gradient (RDG) isosurfaces could exhibit different types of interaction and relative intensities in real space. The RDG function can be expressed as

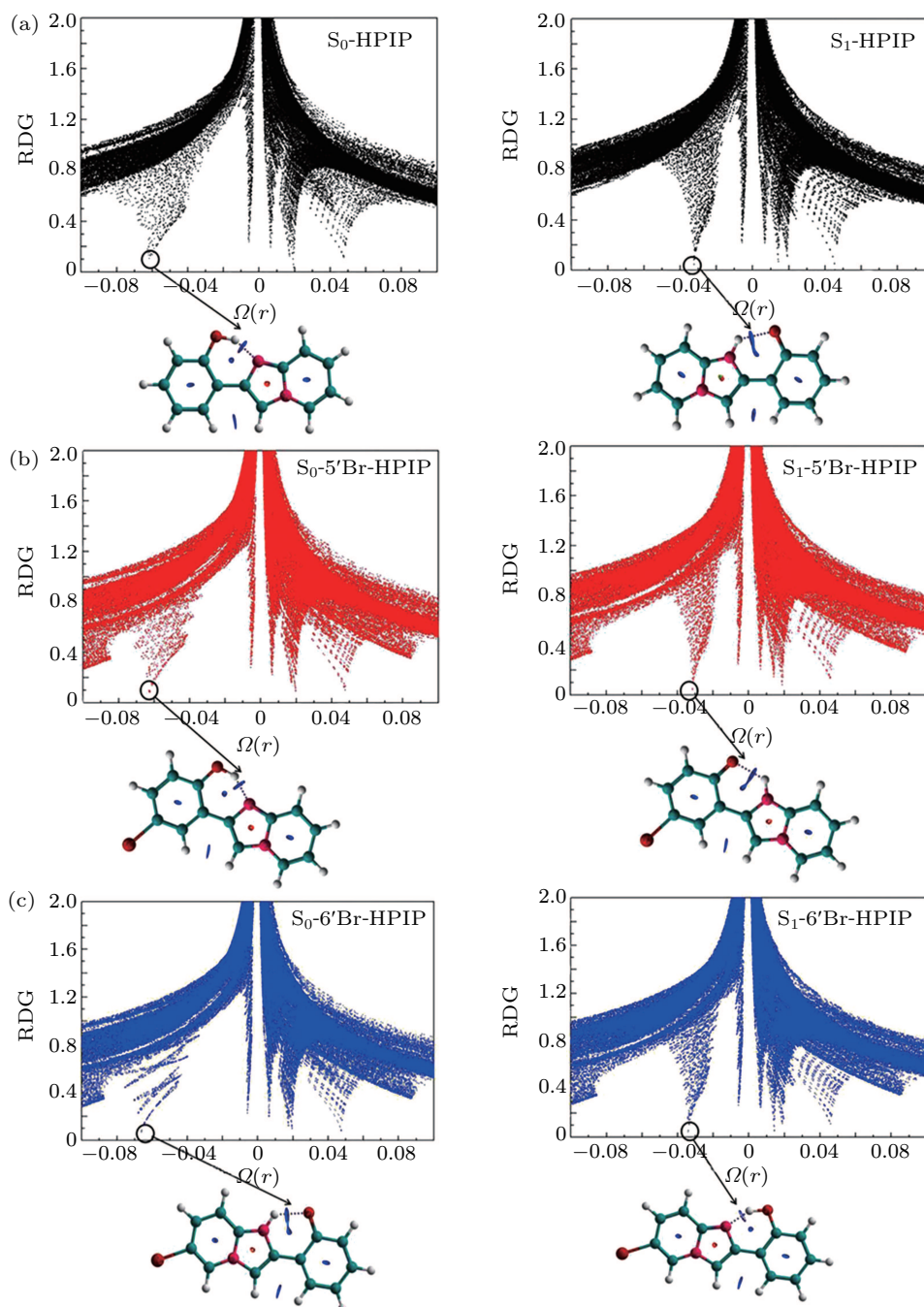$$\mathrm{RDG}(r) = \frac{1}{2(3\pi^2)^{1/3}} \frac{|\nabla\rho(r)|}{\rho(r)^{4/3}}. \tag{1}$$

Moreover, found in Bader's atoms in molecules theory,[48] the second largest eigenvalue λ_2 of the Hessian matrix of electron density and $\rho(r)$ can be connected in

$$\Omega(r) = \mathrm{sign}(\lambda_2(r))\rho(r). \tag{2}$$

The $\lambda_2 > 0$ acts for bonding interactions and the $\lambda_2 < 0$

represents anti-bonding interactions. The $\Omega(r)$ negative value stands for hydrogen bond interaction. And the $\Omega(r)$ is positive for the steric repulsion interaction. The $\Omega(r)$ approaching to zero means van der Waals interaction. The scatter diagrams of $\Omega(r)$ in HPIP, 5′Br-HPIP, and 6′Br-HPIP versus the RDG are plotted in Fig. 3. In S_0 state, the contour value is set as 0.1 for the three molecules, and the spike peak is situated between -0.06 and -0.07. The results showed that the in-

tramolecular hydrogen bond interaction is similar in the three molecules at S_0 state. Moreover, the contour value is set as 0.1 in S_1 state for the three molecules. The spike peak of 5′Br-HPIP (-0.031) and 6′Br-HPIP (-0.035) occured shift relative to HPIP (-0.033). The results of non-covalent interactions greatly supported the fluorescence emission peak results in Fig. 2.

Fig. 3. Plots of $\Omega(r)$ versus RDG for (a) HPIP, (b) 6′Br-HPIP, and (c) 5′Br-HPIP framework in S_0 state and S_1 state, as well as the assignment of each spike by gradient isosurfaces.

3.5. IR spectrum

Infrared vibration spectrum could be used to analyze the proton transfer process by the peak shift of the relevant hydrogen band. Figure 4 displays the calculated IR spectra of HPIP, 5′Br-HPIP, and 6′Br-HPIP. The range of spectrum in ground-state and excited-state was from 2000 cm^{-1}

to 4000 cm^{-1}. As shown in Fig. 4, the vibration frequencies of H–O group in HPIP, 5′Br-HPIP, and 6′Br-HPIP at S$_0$ state were 2853 cm^{-1}, 2813 cm^{-1}, and 2907 cm^{-1}, respectively. In S$_1$ state, the vibration frequencies revealed obviously stretching vibration of N–H, and the vibration frequencies of N–H group in HPIP, 5′Br-HPIP, and 6′Br-HPIP at S$_1$ state were 3583 cm^{-1}, 3552 cm^{-1}, and 3500 cm^{-1}, respectively. For HPIP, 5′Br-HPIP, and 6′Br-HPIP, the original stretching vibration peak (H–O) disappeared, and the new stretching vibration peak (N–H) was explored in the S$_1$ state. In the results, the new vibration peak indicated the ESIPT process occurrence in HPIP, 5′Br-HPIP, and 6′Br-HPIP structures.
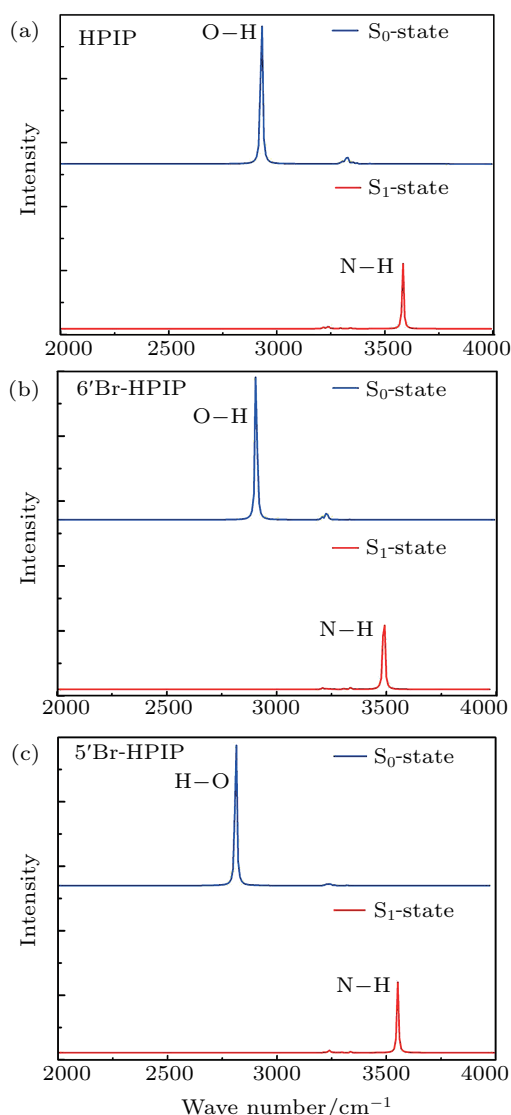

Fig. 4. Calculated IR spectra of (a) HPIP, (b) 6′Br-HPIP, and (c) 5′Br-HPIP in different electronic states. Blue and red lines stand for S$_0$ state and S$_1$ state, respectively.

3.6. Potential energy curve and mechanism analysis

The potential energy curve (PEC) can intuitively reveal the process of proton transfer at the S$_0$ state and S$_1$ state of compounds.[49–52] The potential energy curves of HPIP, 5′Br-HPIP, and 6′Br-HPIP in S$_0$ and S$_1$ states are described in

Fig. 5. In the S$_0$ state, the potential barrier was 7.53 kcal/mol for HPIP, 9.41 kcal/mol for 6′Br-HPIP, and 6.90 kcal/mol for 5′Br-HPIP. And the three molecules in S$_1$ state almost had no energy barrier. The high energy barrier in S$_0$ state indicated that the intramolecular proton transfer (IPT) process can not occur in S$_0$ state spontaneously, and through the photo-excitation to S$_1$ state, the low energy barrier proved that the ESPIT process in S$_1$ state more easily occurred than that in S$_0$ state. The results indicted that the IPT process was initiative for the three molecules in S$_1$ state.
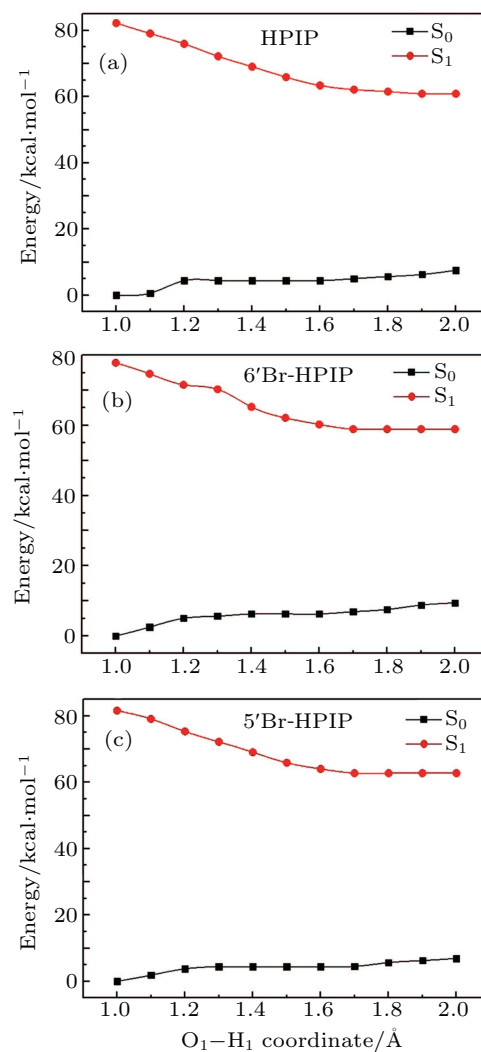

Fig. 5. The potential energy curves of the S$_0$ state and S$_1$ state for (a) HPIP, (b) 6′Br-HPIP, and (c) 5′Br-HPIP.

4. Conclusion

In summary, we theoretically calculated the ESIPT properties of HPIP, 5′Br-HPIP, and 6′Br-HPIP. All theoretical values were consistent with the experimental ones. The IR spectrum in S$_1$ state showed a new N–H peak and the original O–H peak disappeared, which proved the occurrence of ESIPT process. Judging from the results of FMOs, the excited state intramolecular charge transfer (ICT) could influence the ES-IPT process. The potential energy curve in S$_1$ state had no

barrier which indicated that the PT process was spontaneous. From the fluorescence emission spectrum, the ESIPT fluorescence intensity of the three molecules followed the order 5′Br-HPIP>6′Br-HPIP> HPIP. In addition, the ESIPT fluorescence emission peaks of 5′Br-HPIP and 6′Br-HPIP manifested a blue shift and a red shift compared with HPIP, respectively. The different energy gaps of 5′Br-HPIP and 6′Br-HPIP could cause the change of the fluorescence property. And the results of non-covalent interactions corroborated to the results of fluorescence spectrum greatly. Our research on the substituent position influence could be beneficial to design and develop new materials.

Acknowledgment

References

[1] Sato T, Jiang D L and Aida T 1999 *J. Am. Chem. Soc.* **121** 10658
[2] Tong H, Hong Y, Dong Y, Ren Y, Häussler M, Lam J W Y, Wong K S and Tang B Z 2007 *J. Phys. Chem. B* **111** 2000
[3] Kaiser T E, Wang H, Stepanenko V and Würthner F 2007 *Angew. Chem.* **119** 5637
[4] Kaiser T E, Wang H, Stepanenko V and Würthner F 2007 *Angew. Chem. Int. Ed.* **46** 5541
[5] Zhao C H, Wakamiya A, Inukai Y and Yamaguchi S 2006 *J. Am. Chem. Soc.* **128** 15934
[6] Xie Z, Yang B, Li F, Cheng G, Liu L, Yang G, Xu H, Ye L, Hanif M, Liu S, Ma D and Ma Y 2005 *J. Am. Chem. Soc.* **127** 14152
[7] Lupton J M, Hemingway L R, Samuel I D W and Burn P L 2000 *J. Mater. Chem.* **10** 867
[8] Wang J, Zhao Y, Dou C, Sun H, Xu P, Ye K, Zhang J, Jiang S, Li F and Wang Y 2007 *J. Phys. Chem. B* **111** 5082
[9] Luo J, Xie Z, Lam J W Y, Cheng L, Chen H, Qiu C, Kwok H S, Zhan X, Liu Y, Zhu D and Tang B Z 2001 *Chem. Commun.* **18** 1740
[10] Li Y, Li F, Zhang H, Xie Z, Xie W, Xu H, Li B, Shen F, Ye L, Hanif M,Ma D and Ma Y 2007 *Chem. Commun.* 231
[11] Wakamiya A, Mori K and Yamaguchi S 2007 *Angew. Chem.* **119** 4351
[12] Yao H and Funada T 2014 *Chem. Commun.* **50** 2748
[13] El Nahhas A, Pascher T, Leone L, Panzella L, Napolitano A and Sundstrom V 2014 *J. Phys. Chem. Lett.* **5** 2094
[14] Tang K C, Chang M J, Lin T Y, Pan H A, Fang T C, Chen K Y, Hung W Y, Hsu Y H and Chou P T 2011 *J. Am. Chem. Soc.* **133** 17738
[15] Tang K C, Chen C L, Chuang H H, Chen J L, Chen Y J, Lin Y C, Shen J Y, Hu W P and Chou P T 2011 *J. Phys. Chem. Lett.* **2** 3063
[16] Barman S, Mukhopadhyay S K, Biswas S, Nandi S, Gangopadhyay M, Dey S, Anoop A and Singh N D P 2016 *Angew. Chem. Int. Ed.* **55** 4194
[17] Weller A 1956 *Ber. Bunsenges. Phys. Chem.* **60** 1144
[18] Han K L and Zhao G J 2011 *Hydrogen Bonding and Transfer in the Excited State* (Wiley Online Library) p. 464
[19] Amani T, Jordi M, Ali K and Kaher T 2014 *Chin. Phys. B* **23** 46101
[20] Zhou P W and Han K L 2018 *Acc.Chem. Res.* **51** 1681
[21] Zhou P and Zhao L 2018 *Int. J. Quantum Chem.* **118** e25618
[22] Sun C F, Su X, Zhou Q and Shi Y 2019 *Org. Chem. Front.* **6** 3093
[23] Zhao Y, Wang M and Zhou P 2018 *J. Phys. Chem. A* **122** 2864
[24] Zheng J J, Zhang G L, Guo Y X, Li X P and Chen W J 2007 *Chin. Phys. B* **16** 1047
[25] Wu F, Lin L, Li X P, Yu Y X, Zhang G L and Chen W J 2008 *Chin. Phys. B* **17** 1461
[26] Yang D P, Yang G, Zhao J F, Zheng R and Wang Y S 2017 *J. Cluster Sci.* **28** 2449
[27] Zhou P W, Hoffmann M R, Han K L and He G Z 2015 *J. Phys. Chem. B* **119** 2125
[28] Seo J, Kim S and Park S Y 2004 *J. Am. Chem. Soc.* **126** 11154
[29] Han J H, Liu X C, Sun C F, Li Y, Hang Y and Shi Y 2018 *RSC Adv.* **8** 29589
[30] Sun C F, Zhao H F, Liu X C, Yin H and Shi Y 2018 *Org. Chem. Frontiers* **10** 1039
[31] Sakai K i, Takahashi S, Kobayashi A, Akutagawa T, Nakamura T, Dosen M, Kato M and Nagashima U 2010 *Dalton T.* **39** 1989
[32] Zhang X and Liu J Y 2016 *Dyes Pigments* **125** 80
[33] Li Y Q, Yang Y F and Ding Y 2017 *Sci. Rep.* **7** 1574
[34] Bader A N, Pivovarenko V G, Demchenko A P, Ariese F and Gooijer C 2004 *J. Phys. Chem. B* **108** 10589
[35] Wang Y, Yin H, Shi Y, Jin M X and Ding D J 2014 *New J. Chem.* **38** 4458
[36] Zhao J, Chen J, Liu J and Hoffmann M R 2015 *Phys. Chem. Chem. Phys.* **17** 11990
[37] Yasuhiro S, Toshiki M, Hirohiko Hand Koji A 2012 *J. Phys. Chem. A* **116** 12041
[38] Mutai T, Sawatani H, Shida T, Shono H and Araki K 2013 *J. Org. Chem.* **78** 2482
[39] Frisch M J, Trucks G W, Schlegel H B, *et al.* 2009 *Gaussian 09*, Revision B. 01 (Wallingford: Gaussian, Inc.)
[40] Yang Y F, Zhao J F and Li Y Q 2016 *Sci. Rep.* **6** 32152
[41] Zhao J F, Liu X Y and Zheng Y J 2017 *J. Phys. Chem. A* **121** 4002
[42] Yang D P, Yang Y G and Liu Y F 2014 *Spectrochim. Acta Part A* **117** 379
[43] Lu T and Chen F W 2012 *J. Comput. Chem.* **33** 580
[44] https://www.chemcraftprog.com
[45] Liu X C, Yin H, Li H and Shi Y 2017 *Spectrochimica Acta Part A* **77** 1
[46] Contreras-Garcia J, Johnson E R, Keinan S, Chaudret R, Piquemal J P, Beratan D N and Yang W T 2011 *J. Chem. Theory Comput.* **7** 625
[47] Johnson E R, Keinan S, Mori-Sanchez P, Contreras-Carcia J, Cohen A J and Yang W T 2010 *J. Am. Chem. Soc.* **132** 6498
[48] Tang W, Sanville E and Henkelman G 2009 *J. Phys.: Condens Matter* **21** 084204
[49] Li C, Yang Y and Liu Y 2017 *Phys. Chem. Chem. Phys.* **19** 4802
[50] Li C Z, Ma C, Li D L and Liu Y F 2016 *J. Lumin.* **172** 29
[51] Jia L F, Wang F and Liu Y F 2018 *Org. Electron.* **57** 292
[52] Hao J J and Yang Y 2018 *Org. Chem. Front.* **5** 1330